

Dijet correlations in pp collisions at RHIC

Antoni Szczurek*

*Institute of Nuclear Physics, PL-31-342 Cracow, Poland
and University of Rzeszów, PL-35-959 Rzeszów, Poland
E-mail: Antoni.Szczurek@ifj.edu.pl*

Anna Rybarska

*Institute of Nuclear Physics, PL-31-342 Cracow, Poland
E-mail: Anna.Rybarska@ifj.edu.pl*

Gabriela Slipek

*Institute of Nuclear Physics, PL-31-342 Cracow, Poland
E-mail: Gabriela.Slipek@ifj.edu.pl*

We compare results of k_t -factorization approach and next-to-leading order collinear-factorization approach for dijet correlations in proton-proton collisions at RHIC energies. We discuss correlations in azimuthal angle as well as correlations in two-dimensional space of transverse momenta of two jets. Some k_t -factorization subprocesses are included for the first time in the literature. Different unintegrated gluon/parton distributions are used in the k_t -factorization approach. The results depend on UGDF/UPDF used. Limitations due to leading jet condition are discussed.

High- p_T physics at LHC

March 23-27 2007

University of Jyväskylä, Jyväskylä, Finland

*Speaker.

1. Introduction

The jet correlations are interesting in the context of recent detailed studies of hadron-hadron correlations in nucleus-nucleus [1] and proton-proton [2] collisions. Those studies provide interesting information on the dynamics of nuclear and elementary collisions. Effects of geometrical jet structure were discussed recently in Ref.[3]. No QCD calculation of parton radiation was performed up to now in this context. Before going into hadron-hadron correlations it seems indispensable to better understand correlations between jets due to the QCD radiation. In this paper we address the case of elementary hadronic collisions in order to avoid complicated and not yet well understood nuclear effects. Our analysis should be considered as a first step in order to understand the nuclear case in the future. In leading-order collinear-factorization approach jets are produced back-to-back. These leading-order jets are therefore not included into correlation function, although they contribute a big ($\sim \frac{1}{2}$) fraction to the inclusive cross section.

The truly internal momentum distribution of partons in hadrons due to Fermi motion (usually neglected in the literature) and/or any soft emission would lead to a decorrelation from the simple kinematical back-to-back configuration. In the fixed-order collinear approach only next-to-leading order terms lead to nonvanishing cross sections at $\phi \neq \pi$ and/or $p_{1,t} \neq p_{2,t}$ (moduli of transverse momenta of outgoing partons). In the k_t -factorization approach, where transverse momenta of gluons entering the hard process are included explicitly, the decorrelations come naturally in a relatively easy to calculate way. In Fig.1 we show k_t -factorization processes discussed up to now in the literature [5, 6, 7]. The soft emissions, not explicit in our calculation, are hidden in model unintegrated gluon distribution functions (UGDF). In our calculation the last objects are assumed to be given and are taken from the literature [8, 9, 10].

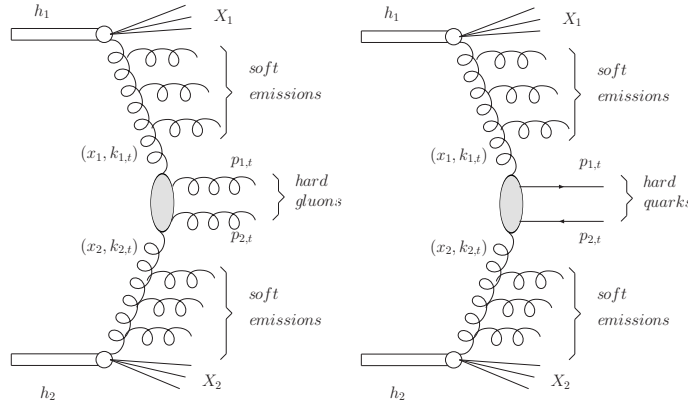


Figure 1: Diagrams for k_t -factorization approach included in the literature. We shall call them A_1 and A_2 for brevity.

In addition we include two new processes (see Fig.2), not discussed up to now in the context of k_t -factorization approach. We shall discuss their role at the RHIC energy $W = 200$ GeV.

Furthermore we compare results obtained within the k_t -factorization approach and results obtained in the NLO collinear-factorization. Here we wish to address the problem of the relation between both approaches. We shall identify the regions of the phase space where the hard $2 \rightarrow 3$

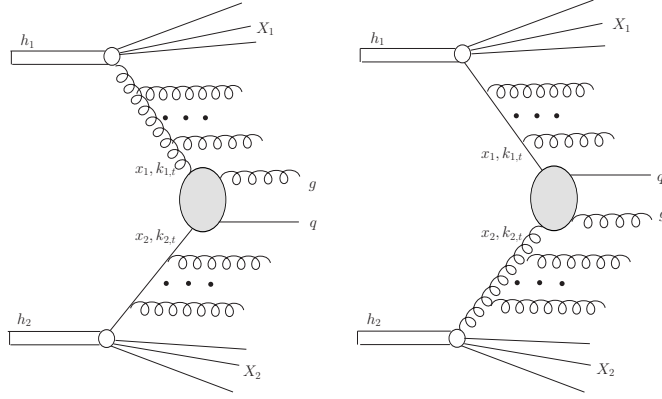


Figure 2: Diagrams for k_t -factorization approach included for the first time here. We shall call them B_1 and B_2 for brevity.

processes, not explicitly included in the leading-order k_t -factorization approach, dominate over the $2 \rightarrow 2$ contributions calculated with UGDFs. We shall show how the results depend on UGDFs used.

We shall concentrate on the region of relatively semi-hard jets, i.e. on the region related to the recently measured hadron-hadron correlations at RHIC.

2. Formalism

The cross section for the production of a pair of partons (k,l) can be written as

$$\frac{d\sigma(h_1 h_2 \rightarrow jet\ jet)}{d^2 p_{1,t} d^2 p_{2,t}} = \sum_{i,j,k,l} \int dy_1 dy_2 \frac{d^2 k_{1,t}}{\pi} \frac{d^2 k_{2,t}}{\pi} \frac{1}{16\pi^2 (x_1 x_2 s)^2} |\overline{\mathcal{M}}(ij \rightarrow kl)|^2 \cdot \delta^2(\vec{k}_{1,t} + \vec{k}_{2,t} - \vec{p}_{1,t} - \vec{p}_{2,t}) \mathcal{F}_i(x_1, k_{1,t}^2) \mathcal{F}_j(x_2, k_{2,t}^2), \quad (2.1)$$

where

$$x_1 = \frac{m_{1,t}}{\sqrt{s}} e^{+y_1} + \frac{m_{2,t}}{\sqrt{s}} e^{+y_2}, \quad (2.2)$$

$$x_2 = \frac{m_{1,t}}{\sqrt{s}} e^{-y_1} + \frac{m_{2,t}}{\sqrt{s}} e^{-y_2}, \quad (2.3)$$

and $m_{1,t}$ and $m_{2,t}$ are so-called transverse masses defined as $m_{i,t} = \sqrt{p_{i,t}^2 + m^2}$, where m is the mass of a parton. In the following we shall assume that all partons are massless. The objects denoted by $\mathcal{F}_i(x_1, k_{1,t}^2)$ and $\mathcal{F}_j(x_2, k_{2,t}^2)$ in the equation (2.1) above are the unintegrated parton distributions in hadron h_1 and h_2 , respectively. They are functions of longitudinal momentum fraction and transverse momentum of the incoming (virtual) parton.

After some simple algebra one obtains a handy formula:

$$\frac{d\sigma(p_{1,t}, p_{2,t})}{dp_{1,t} dp_{2,t}} = \frac{1}{2} \cdot \frac{1}{2} \cdot 4\pi \int d\phi_- p_{1,t} p_{2,t} \sum_{i,j,k,l} \int dy_1 dy_2 \frac{1}{4} q_i dq_t d\phi_{q_i} \left(\frac{1}{16\pi^2 (x_1 x_2 s)^2} |\overline{\mathcal{M}}(ij \rightarrow kl)|^2 \mathcal{F}_i(x_1, k_{1,t}^2) \mathcal{F}_j(x_2, k_{2,t}^2) \right), \quad (2.4)$$

where ϕ_- is a relative azimuthal angle between outgoing partons (jets) and $\vec{q}_t = \vec{k}_{1,t} - \vec{k}_{2,t}$ is a new auxiliary vector variable.

This 5-dimensional integral is now calculated for each point on the map $p_{1,t} \times p_{2,t}$.

Up to now we have considered only processes with two explicit hard partons. Now we shall discuss also processes with three explicit hard partons. In Fig.3 we show a typical $2 \rightarrow 3$ process and kinematical variables needed in the description of the process. We select the particle 1 and 2 as those which correlations are studied. This is only formal as all possible combinations are considered in real calculations.

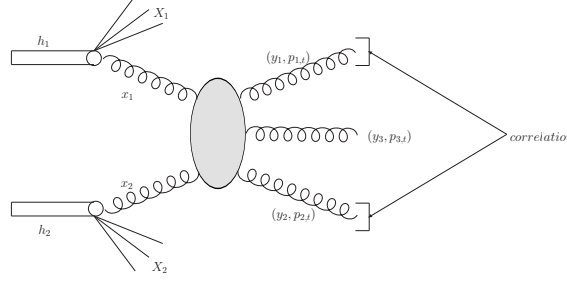


Figure 3: A typical $2 \rightarrow 3$ process. The kinematical variables used are shown explicitly.

The cross section for $h_1 h_2 \rightarrow g g g X$ can be calculated according to the standard parton model formula:

$$d\sigma(h_1 h_2 \rightarrow g g g) = \int dx_1 dx_2 g_1(x_1, \mu^2) g_2(x_2, \mu^2) d\hat{\sigma}(g g \rightarrow g g g), \quad (2.5)$$

where the longitudinal momentum fractions are evaluated as

$$\begin{aligned} x_1 &= \frac{p_{1,t}}{\sqrt{s}} \exp(+y_1) + \frac{p_{2,t}}{\sqrt{s}} \exp(+y_2) + \frac{p_{3,t}}{\sqrt{s}} \exp(+y_3), \\ x_2 &= \frac{p_{1,t}}{\sqrt{s}} \exp(-y_1) + \frac{p_{2,t}}{\sqrt{s}} \exp(-y_2) + \frac{p_{3,t}}{\sqrt{s}} \exp(-y_3). \end{aligned} \quad (2.6)$$

After a simple algebra [4] we get finally:

$$d\sigma = \frac{1}{64\pi^4 s^2} x_1 g_1(x_1, \mu_f^2) x_2 g_2(x_2, \mu_f^2) |\overline{\mathcal{M}}_{2 \rightarrow 3}|^2 p_{1,t} dp_{1,t} p_{2,t} dp_{2,t} d\phi_- dy_1 dy_2 dy_3, \quad (2.7)$$

where ϕ_- is restricted to the interval $(0, \pi)$. The last formula is very useful in calculating the cross section for particle 1 and particle 2 correlations. The soft and collinear singularities are removed by imposing an extra jet (parton) cone separation condition for each dijet pair with the jet-cone radius being a free parameter.

3. Results

Let us concentrate first on $2 \rightarrow 2$ processes calculated within k_t -factorization approach.

In Fig.4 we show two-dimensional maps in $(p_{1,t}, p_{2,t})$ for all k_t -factorization processes shown in Fig.1 and Fig.2. Only very few approaches in the literature include both gluons and quarks and

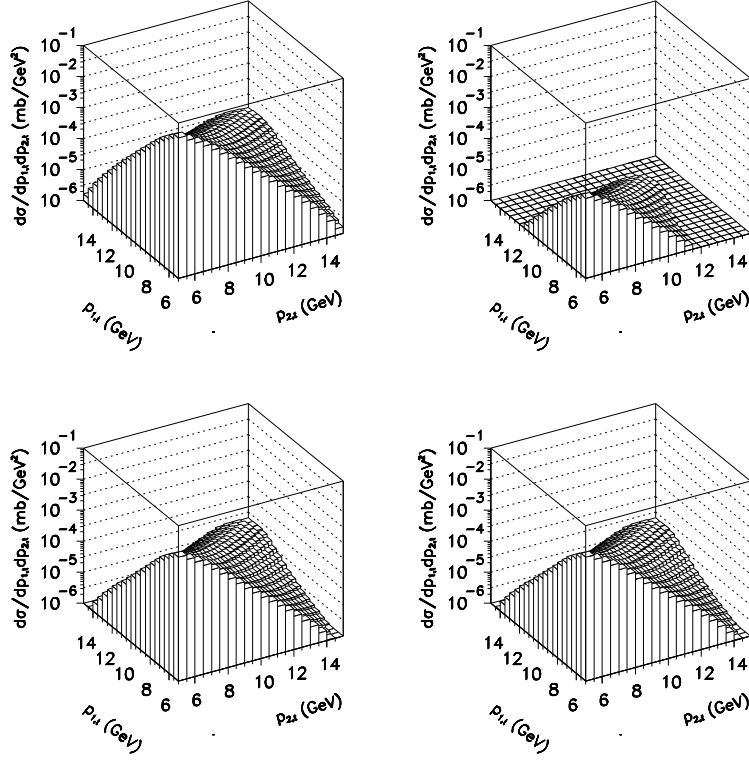


Figure 4: Two-dimensional distributions in $p_{1,t}$ and $p_{2,t}$ for different subprocesses $gg \rightarrow gg$ (left upper) $gg \rightarrow q\bar{q}$ (right upper), $gq \rightarrow gq$ (left lower) and $qg \rightarrow qg$ (right lower). In this calculation $W = 200$ GeV and Kwieciński UPDFs with exponential nonperturbative form factor ($b_0 = 1$ GeV $^{-1}$) and $\mu^2 = 100$ GeV 2 were used. Here integration over full range of parton rapidities was made.

antiquarks. In the calculation above we have used Kwieciński UPDFs with exponential nonperturbative form factor ($b_0 = 1$ GeV $^{-1}$) and the factorization scale $\mu^2 = (p_{t,min} + p_{t,max})^2/4 = 100$ GeV 2 .

In Fig.5 we show fractional contributions (individual component to the sum of all four components) of the above four processes on the two-dimensional map (y_1, y_2) . One point here requires a better clarification. Experimentally it is not possible to distinguish gluon and quark/antiquark jets. Therefore in our calculation of the (y_1, y_2) dependence one has to symmetrize the cross section (not the amplitude) with respect to gluon – quark/antiquark exchange ($y_1 \rightarrow y_2, y_2 \rightarrow y_1$). While at midrapidities the contribution of diagram $B_1 + B_2$ is comparable to the diagram A_1 , at larger rapidities the contributions of diagrams of the type B dominate. The contribution of diagram A_2 is relatively small in the whole phase space. When calculating the contributions of the diagram A_1 and A_2 one has to be careful about collinear singularity which leads to a significant enhancement of the cross section at $\phi_- = 0$ and $y_1 = y_2$, i.e. in the one jet case, when both partons are emitted in the same direction. This is particularly important for the matrix elements obtained by the naive analytic continuation from the formula for on-shell initial partons. The effect can be, however, easily eliminated with the jet-cone separation algorithm [4].

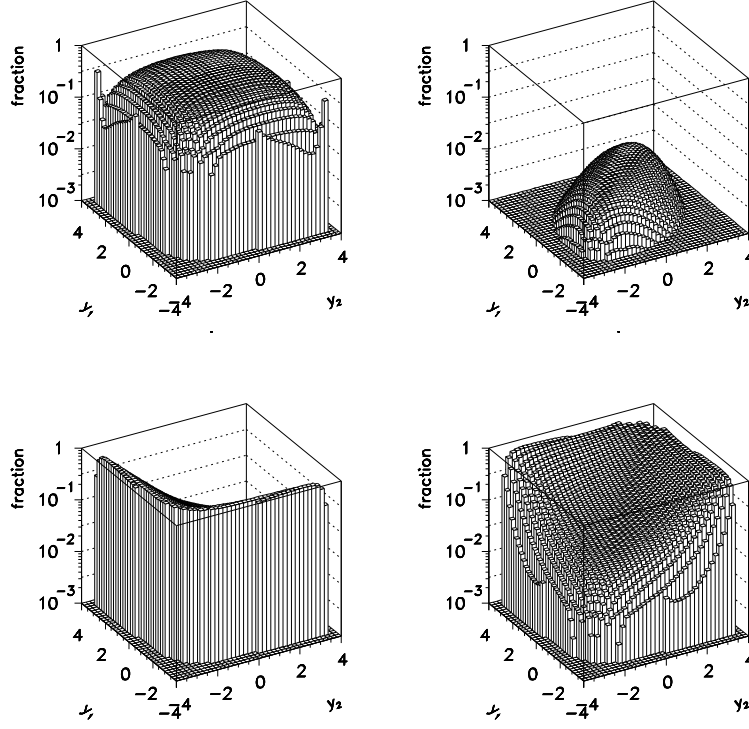


Figure 5: Two-dimensional distributions of fractional contributions of different subprocesses as a function of y_1 and y_2 for $gg \rightarrow gg$ (left upper) $gg \rightarrow q\bar{q}$ (right upper), $gq \rightarrow gq$ (left lower) and $qg \rightarrow qg$ (right lower). In this calculation $W = 200$ GeV and Kwieciński UPDFs with exponential nonperturbative form factor and $b_0 = 1$ GeV $^{-1}$ were used. The integration is made for jets from the transverse momentum interval: $5 \text{ GeV} < p_{1,t}, p_{2,t} < 20 \text{ GeV}$.

For completeness in Fig.6 we show azimuthal angle dependence of the cross section for all four components. There is no sizeable difference in the shape of azimuthal distribution for different components.

The Kwieciński approach allows to separate the unknown perturbative effects incorporated via nonperturbative form factors and the genuine effects of QCD evolution. The Kwieciński distributions have two external parameters:

- the parameter b_0 responsible for nonperturbative effect (for details see [4]),
- the evolution scale μ^2 (for details see [4]).

While the latter can be identified physically with characteristic kinematical quantities in the process $\mu^2 \sim p_{1,t}^2, p_{2,t}^2$, the first one is of nonperturbative origin and cannot be calculated from first principles. The shapes of distributions depends, however, strongly on the value of the parameter b_0 in which the initial momentum distribution is encoded. This is demonstrated in Fig.7 where we show angular correlations in azimuth for the $gg \rightarrow gg$ subprocess. The smaller b_0 the bigger decorrelation in azimuthal angle can be observed. In Fig.7 we show also the role of the evolution

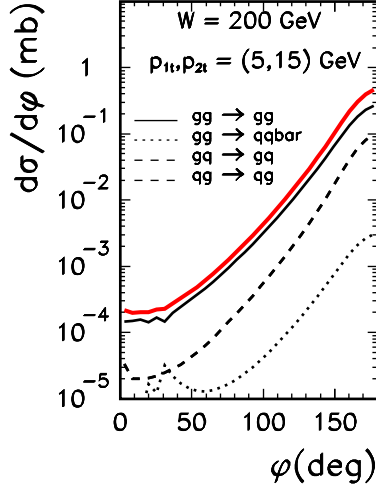


Figure 6: The angular correlations for all four components: $gg \rightarrow gg$ (solid), $gg \rightarrow q\bar{q}$ (dashed) and $qg \rightarrow gq = qg \rightarrow qg$ (dash-dotted). The calculation is performed with the Kwieciński UPDFs and $b_0 = 1 \text{ GeV}^{-1}$. The integration is made for jets from the transverse momentum interval: $5 \text{ GeV} < p_{1,t}, p_{2,t} < 15 \text{ GeV}$ and from the rapidity interval: $-4 < y_1, y_2 < 4$.

scale in the Kwieciński distributions. The QCD evolution embedded in the Kwieciński evolution equations populate larger transverse momenta of partons entering the hard process. This significantly increases the initial (nonperturbative) decorrelation in azimuth. For transverse momenta of the order of $\sim 10 \text{ GeV}$ the effect of evolution is of the same order of magnitude as the effect due to the nonperturbative physics of hadron confinement. For larger scales of the order of $\mu^2 \sim 100 \text{ GeV}^2$, more adequate for jet production, the initial condition is of minor importance and the effect of decorrelation is dominated by the evolution. Asymptotically (infinite scales) there is no dependence on the initial condition provided reasonable initial conditions are taken.

In Fig.8 we show the maps for different UGDFs and for $gg \rightarrow ggg$ processes in the broad range of transverse momenta $5 \text{ GeV} < p_{1,t}, p_{2,t} < 20 \text{ GeV}$ for the RHIC energy $W = 200 \text{ GeV}$. In this calculation we have not imposed any particular cuts on rapidities. We have not imposed also any cut on the transverse momentum of the unobserved third jet in the case of $2 \rightarrow 3$ calculation. The small transverse momenta of the third jet contribute to the sharp ridge along the diagonal $p_{1,t} = p_{2,t}$. No extra cut for the $gg \rightarrow ggg$ contribution (right lower panel) means a singularity along the diagonal $p_{1,t} = p_{2,t}$ which is, however, not visible in the figure because of a finite grid of mesh points and because of the way of selecting the mesh points (no points on the diagonal). Naturally it is rather difficult to distinguish the three-parton states from standard two jet events. In principle, the ridge can be eliminated by imposing a cut on the transverse momentum of the third (unobserved) parton [4]. There are also other methods to eliminate the ridge and underlying soft processes which is discussed in Ref.[4].

When calculating dijet correlations in the standard NLO ($2 \rightarrow 3$) approach we have taken all possible dijet combinations. This is different from what is usually taken in experiments [11], where correlation between leading jets are studied. In our notation this means $p_{3,t} < p_{1,t}$ and $p_{3,t} < p_{2,t}$.

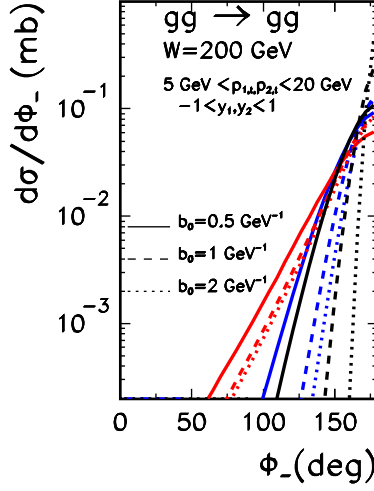


Figure 7: The azimuthal correlations for the $gg \rightarrow gg$ component obtained with the Kwieciński UGDFs for different values of the nonperturbative parameter b_0 and for different evolution scales $\mu^2 = 10$ (on line blue), 100 (on line red) GeV^2 . The initial distributions (without evolution) are shown for reference by black lines.

When imposing such extra condition on our NLO calculation we get the dash-dotted curve in Fig.9. In this case $d\sigma/d\phi_- = 0$ for $\phi_- < 2/3\pi$. This vanishing of the cross section is of purely kinematical origin. Since in the k_t -factorization calculation only two jets are explicit, there is no such an effect in this case. This means that the region of $\phi_- < 2/3\pi$ should be useful to test models of UGDFs. For completeness in Fig.10 we show a two-dimensional plot $(p_{1,t}, p_{2,t})$ with imposing the leading-jet condition. Surprisingly the leading-jet condition removes a big part of the two-dimensional space. In particular, regions with $p_{2,t} > 2p_{1,t}$ and $p_{1,t} > 2p_{2,t}$ cannot be populated via $2 \rightarrow 3$ subprocess¹. There are no such limitations for $2 \rightarrow 4$, $2 \rightarrow 5$ and even higher-order processes. Therefore measurements in “NLO-forbidden” regions of the $(p_{1,t}, p_{2,t})$ plane would test higher-order terms of the standard collinear pQCD. These are also regions where UGDFs can be tested, provided that not too big transverse momenta of jets are taken into the correlation in order to assure the dominance of gluon-initiated processes. For larger transverse momenta and/or forward/backward rapidities one has to include also quark/antiquark initiated processes via unintegrated quark/antiquark distributions.

4. Summary

Motivated by the recent experimental results of hadron-hadron correlations at RHIC we have discussed dijet correlations in proton-proton collisions. We have considered and compared results obtained with collinear next-to-leading order approach and leading-order k_t -factorization approach.

In comparison to recent works in the framework of k_t -factorization approach, we have included two new mechanisms based on $gq \rightarrow gq$ and $qg \rightarrow qg$ hard subprocesses. This was done based

¹In LO collinear approach the whole plane, except of the diagonal $p_{1,t} = p_{2,t}$, is forbidden.

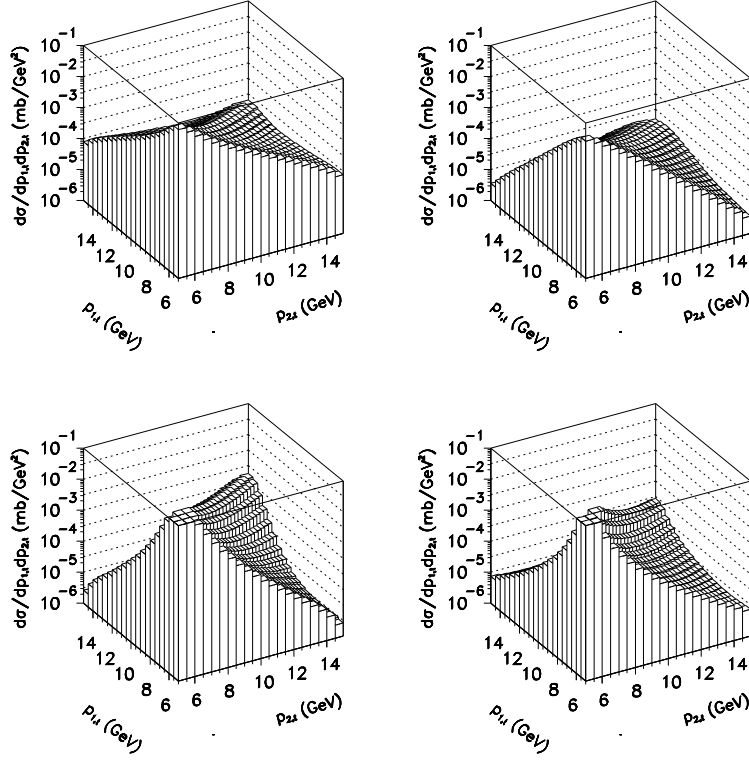


Figure 8: Two-dimensional distributions in p_{1t} and p_{2t} for KL (left upper), BFKL (right upper), Ivanov-Nikolaev (left lower) UGDFs and for the $gg \rightarrow ggg$ (right lower). In this calculation $-4 < y_1, y_2 < 4$.

on the Kwieciński unintegrated parton distributions. We find that the new terms give significant contribution at RHIC energies. In general, the results of the k_t -factorization approach depend on UGDFs/UPDFs used, i.e. on approximation and assumptions made in their derivation.

The results obtained in the standard NLO approach depend significantly whether we consider correlations of any jets or correlations of only leading jets. In the NLO approach one obtains $\frac{d\sigma}{d\phi_-} = 0$ if $\phi_- < 2/3\pi$ for leading jets as a result of a kinematical constraint. Similarly $\frac{d\sigma}{dp_{1,t}dp_{2,t}} = 0$ if $p_{1,t} > 2p_{2,t}$ or $p_{2,t} > 2p_{1,t}$.

There is no such a constraint in the k_t -factorization approach which gives a nonvanishing cross section at small relative azimuthal angles between leading jets and transverse-momentum asymmetric configurations. We conclude that in these regions the k_t -factorization approach is a good and efficient tool for the description of leading-jet correlations. Rather different results are obtained with different UGDFs which opens a possibility to verify them experimentally. Alternatively, the NLO-forbidden configurations can be described only by higher-order (NNLO and higher-order) terms. We do not need to mention that this is a rather difficult and technically involved computation.

What are consequences for particle-particle correlations measured recently at RHIC requires a separate dedicated analysis. Here the so-called leading particles may come both from leading and non-leading jets. This requires taking into account the jet fragmentation process.

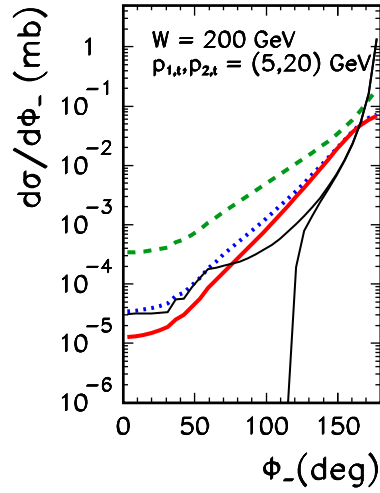


Figure 9: Dijet azimuthal correlations $d\sigma/d\phi_-$ for the $gg \rightarrow gg$ component and different UGDFs as a function of azimuthal angle between the gluonic jets. In this calculation $W = 200$ GeV and $-1 < y_1, y_2 < 1$, $5 \text{ GeV} < p_{1,t}, p_{2,t} < 20 \text{ GeV}$. Here the thick-solid line corresponds to the Kwieciński UGDF, the dashed line to the Kharzeev-Levin type of distribution and the dotted line to the BFKL distribution. The two thin solid (on line black) lines are for NLO collinear approach without (upper line) and with (lower line) leading jet restriction.

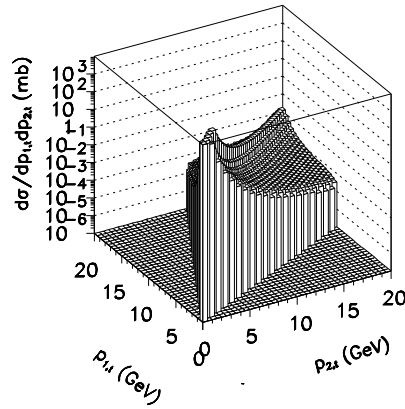


Figure 10: Cross section for the $gg \rightarrow ggg$ component on the $(p_{1,t}, p_{2,t})$ plane with the condition of leading jets (partons).

Acknowledgments This work is partially supported by the grant of the Polish Ministry of Scientific Research and Information Technology number 1 P03B 028 28.

References

- [1] S.S. Adler et al. (PHENIX collaboration), Phys. Rev. Lett. **97** (2006) 052301;
S.S. Adler et al. (PHENIX collaboration), Phys. Rev. **C73** (2006) 054903;

- S.S. Adler et al. (PHENIX collaboration), Phys. Rev. Lett. **96** (2006) 222301;
M. Oldenburg et al. (STAR collaboration), Nucl. Phys. **A774** (2006) 507.
- [2] S.S. Adler et al. (PHENIX collaborations), Phys. Rev. **D74** (2006) 072002.
- [3] P. Levai, G. Fai and G. Papp, Phys. Lett. **B634** (2006) 383.
- [4] A. Szczurek, A. Rybarska and G. Ślipek, arXiv:0704.3537.
- [5] A. Leonidov and D. Ostrovsky, Phys. Rev. **D62** (2000) 094009.
- [6] D. Ostrovsky, Phys. Rev. **D62** (2000) 054028.
- [7] J. Bartels, A. Sabio Vera and F. Schwennsen, hep-ph/0608154, JHEP 0611 (2006) 051.
- [8] D. Kharzeev and E. Levin, Phys. Lett. **B523** (2001) 79.
- [9] A.J. Askew, J. Kwieciński, A.D. Martin and P.J. Sutton, Phys. Rev. **D49** (1994) 4402.
- [10] J. Kwieciński, Acta Phys. Polon. **B33** (2002) 1809;
A. Gawron and J. Kwieciński, Acta Phys. Polon. **B34** (2003) 133;
A. Gawron, J. Kwieciński and W. Broniowski, Phys. Rev. **D68** (2003) 054001.
- [11] V.M. Abazov et al. (D0 collaboration), Phys. Rev. Lett. **94** (2005) 221801.